Journal of Testing and Evaluation, Vol. 35, No. 4
Paper ID JTE100688
Available online at: www.astm.org

M. Brieu,[1] *J. Diani,*[2] *and N. Bhatnagar*[3]

A New Biaxial Tension Test Fixture for Uniaxial Testing Machine—A Validation for Hyperelastic Behavior of Rubber-like Materials

ABSTRACT: A new mechanism for a biaxial tension test is developed for loading an in-plane specimen simultaneously in two principal directions. This mechanism can be adapted to any uniaxial tension test machine and thereby it reduces the cost of conducting tests on expensive machines. It provides a uniform state of equibiaxial tension necessary for procedure characterizing the biaxial loading of any material system and particularly for understanding the hyperelastic behavior law of rubber-like materials for large deformations. The mechanism can also be utilized for evaluating an interaction coefficient of anisotropic or orthotropic materials like reinforced composites that can help in characterizing and predicting failure behavior. As a sample case, the experimental results obtained by this new mechanism are validated with the existing models for two rubber-like materials undergoing hyperelasticity.

KEYWORDS: biaxial tensile, uniaxial test, hyperelastic, rubber-like materials, large deformation

Introduction

The characterization of hyperelastic mechanical behavior of rubber-like materials is one of the essential preliminaries for the design of structures using such materials. The isotropic rubber-like materials hyperelastic behavior is defined by a strain energy density as seen in Refs. [1–4], among others depending on the right Cauchy-Green invariants [1].

The use of only the uniaxial tensile test for the characterization of such strain energy density is insufficient as discussed by earlier researchers [5–11]. A second mechanical test, using several directions of stretching, is generally required. Among the various mechanical tests available, the pure shear and the biaxial tensile tests are the most widely used. The main drawback of the pure hear test is low stretching that does exist. The biaxial tensile test induces a large variation of the strain invariants as compared to the uniaxial tension test. For this reason the biaxial tension test is often carried out [5–8,10,12]. In order to carry out the biaxial tensile test successfully, several mechanisms were proposed earlier [2,3,5–8,10,13–16]. However, several difficulties were encountered in using such devices and mechanisms and as a result, the biaxial experimental data are almost negligible in the literature compared to other test data of not only hyperelastic materials but also reinforced composite materials. Also, it is well known from Mullins' work Refs. [17,18] that rubber-like materials undergo strain-induced stress softening during the first loading. To reach hyperelasticity, a cyclic preloading is applied before stress and strain are measured. The amount of strain-induced stress softening depends on the amount of applied strain during the preloading. Therefore, it is vital to make controlled cyclic loadings in any biaxial tension test to get reasonable characteristic experimental data.

In order to assess the reliability of a proposed strain energy density function and its closeness to experimental data, it is also imperative to compare the already identified strain energy density on a third mechanical test. Most of the time, the third test is carried out for pure shear. But for these hyperelastic materials, pure shear response is close to a uniaxial tension test. Therefore, pure shear does not seem to be the best mechanical test to perform in order to validate a strain energy density; rather it seems interesting to carry out a biaxial test which could induce a load highly different from the response obtained by the earlier mechanical tests carried out in order to identify a strain energy density.

In the present paper, a new mechanism of biaxial tension for large deformation is proposed which can be adapted to any uniaxial tension test machine and which can carry out a biaxial tensile test with, if required, different stretch ratios in the two directions of in-plane extension. The interest of such a mechanism is illustrated through the validation of phenomenological behavior laws on experimental data. After introducing the hyperelastic behavior of rubber-like materials, some classical strain energy density functions, which fit such behavior, are also reported. Parameter identification of strain energy densities is then briefly described. The shortcomings of the already existing biaxial devices are discussed and compared with the proposed new mechanism of biaxial tension for large deformation. The new mechanism allows equibiaxial tension and also the biaxial tension test with different deformations in both the extended directions. Finally, the strain energy densities are validated with the help of experimental data. Some strain energy density parameters are further calculated on a uniaxial and then on an equibiaxial extension test and are then compared to justify the advantage of the new mechanism.

Manuscript received June 8, 2006; accepted for publication October 25, 2006; published online December 2006.

[1]LML—Ecole Centrale de Lille—Cité Scientifique B.P. 48-59651 Villeneuve d'Ascq CEDEX, France, e-mail: mathias.brieu@ec-lille.fr

[2]LIM—ENSAM de Paris, 151 bd de l'hôpital, 75013 Paris, France

[3]Department of Mechanical Engineering, Indian Institute of Technology—Delhi, New Delhi 110016, India, e-mail: nareshb@mech.iitd.ernet.in

Hyperelastic Behavior of Rubber-Like Materials

Strain Energy Density

In order to represent the hyperelastic behavior of a rubber-like material, one has to define a strain energy density W from which the constitutive equation can be derived in terms of:

$$\underline{\underline{\tau}} = \frac{\partial W(\underline{\underline{F}})}{\partial \underline{\underline{F}}} \tag{1}$$

where, $\underline{\underline{\tau}}$ is the first Piola-Kirchhoff stress tensor and $\underline{\underline{F}}$ is the deformation gradient tensor. If the material is assumed to be isotropic, W can be written in terms of the right Cauchy-Green tensor, $\underline{\underline{C}}=\underline{\underline{F}}^T\underline{\underline{F}}$, strain invariants [1]:

$$I_1 = tr(\underline{\underline{C}}); \quad I_2 = \frac{1}{2}((tr\underline{\underline{C}})^2 - tr(\underline{\underline{C}}^2)); \quad I_3 = \det(\underline{\underline{C}}) \tag{2}$$

In such conditions Eq. 1 becomes:

$$\underline{\underline{\tau}} = \frac{\partial W(I_1,I_2,I_3)}{\partial \underline{\underline{F}}} = 2\left[\frac{\partial W}{\partial I_1}\underline{\underline{F}} + \frac{\partial W}{\partial I_2}(I_1\underline{\underline{F}} - \underline{\underline{F}}\,\underline{\underline{C}}) + \frac{\partial W}{\partial I_3}I_3\underline{\underline{F}}^{-T}\right] \tag{3}$$

The part $\partial W/\partial I_3$ in Eq. 3 characterizes the compressible behavior of rubber-like materials while the two other derived parts of W characterize the incompressible behavior. While the dependence of W on I_3 is usually defined through a compression test [19] the other part of the function is obtained assuming that the material is incompressible. Most of the engineering elastomers are slightly compressible materials, the ratio of shear modulus over bulk modulus being of the order of 10^{-4}. Volume changes, at ambient pressure and in many practically important loading conditions such as uniaxial tension, biaxial tension, and shear loadings differ from unity to about 10^{-4} [20]. Hence, incompressibility is usually assumed when characterizing the incompressible part of W. In such conditions, Eq. 3 could transform to:

$$\underline{\underline{\tau}} = 2\left[\frac{\partial W(I_1,I_2)}{\partial I_1}\underline{\underline{F}} + \frac{\partial W(I_1,I_2)}{\partial I_2}(I_1\underline{\underline{F}} - \underline{\underline{F}}\,\underline{\underline{C}})\right] - p\underline{\underline{F}}^{-t} \tag{4}$$

where p is a Lagrange multiplier. In this equation, the deformation gradient tensor $\underline{\underline{F}}$ is assumed such that $\det(\underline{\underline{F}})=1$.

Strain Energy Density Functions

There are two different approaches to describe the behavior of rubber-like materials, the macromolecular models and the phenomenological approach.

In the first case, rubber-like materials are described in a macromolecular network made with very long and flexible chains [21,22]. Several works are published [23–29] among others which allow curve fitting of experimental data with some success. These laws have an advantage of depending on physically related parameters but are usually less effective than the phenomenological behavior laws.

In the second approach, the isotropic hyperelastic behavior of rubber-like materials is represented by the use of an arbitrary strain energy density function depending only on strain invariants. Some of the key contributions to this approach are seen in Refs. [1–3,11,30,31]. Although such strain energy densities have been proven to give very good results even for large strains [2,3,11], it usually depends on many parameters and a parameter identification procedure is always desirable.

Identification of Strain Energy Density Functions

The parameter identification procedure is discussed briefly based on the work of Lambert-Diani and Rey [11].

In order to determine the stress-strain relation, Eq. 4, both the functions, $\partial W/\partial I_1$ and $\partial W/\partial I_2$ are required. From the work of Kawabata et al. [9,10] who proved that $\partial W/\partial I_1$ and $\partial W\partial I_2$ depend only on I_1, and I_2, respectively, and from the work of Fukahori and Seki [10] it was shown that $\partial W/\partial I_2$ was negligible in the case of the uniaxial tension test. Lambert-Diani and Rey [11] proposed to identify $\partial W/\partial I_1$ based on the uniaxial tension test, assuming $\partial W/\partial I_2=0$. Once $\partial W/\partial I_1$ is identified then $\partial W/\partial I_2$ could be determined by an equibiaxial tension test. Hence, the parameter identification procedure requires a uniaxial tension test and an equibiaxial test. Considering uniaxial tension for which $\underline{\underline{F}} = Diag(\lambda, \lambda^{-1/2}, \lambda^{-1/2})$, and equibiaxial tension for which $\underline{\underline{F}} = Diag(\lambda, \lambda, \lambda^{-2})$, and using Eq. 4, the nonzero stress in both cases of loadings could be evaluated by using the following expression:

$$\begin{aligned} T_{11}^{UT} &= 2\left(\frac{\partial W}{\partial I_1}\left(\lambda - \frac{1}{\lambda^2}\right) + \frac{\partial W}{\partial I_2}\left(1 - \frac{1}{\lambda^3}\right)\right) \\ T_{11}^{EBT} &= 2\left(\frac{\partial W}{\partial I_1}\left(\lambda - \frac{1}{\lambda^5}\right) + \frac{\partial W}{\partial I_2}\left(\lambda^3 - \frac{1}{\lambda^3}\right)\right) \end{aligned} \tag{5}$$

where T_{11} is the nominal stress in the vertical direction, superscript UT is for uniaxial tension, and EBT is equibiaxial tension.

Two different strain energy functions proposed in the literature, which are considered to provide a good correlation between experiments and the model are given below. The first one was proposed by Harth-Smith [2] and is defined by:

$$W^{HS}(I_1,I_2) = C_1\int_3^{I_1} \exp(C_3(I_1-3)^2)dI_1 + C_2 \ln\frac{I_2}{3} \tag{6}$$

and the second one was proposed by Lambert-Diani and Rey [11] and is defined by:

$$\begin{aligned} W^{DR}(I_1,I_2) = &\int_3^{I_1} \exp(\alpha_0 + \alpha_1(I_1-3) + \alpha_2(I_1-3)^2)dI_1 \\ &+ \int_3^{I2} \beta_0 I_2^{\beta_1} dI_2 \end{aligned} \tag{7}$$

A New Biaxial Tension Fixture

The Existing Equibiaxial Tension Machine

Biaxial tension tests are complex to carry out; however, they are a must for evaluating the strain energy density functions. First, the existing mechanisms are discussed and then a new experimental mechanism is proposed which can allow one to carry out equibiaxial and also biaxial tension tests with different loadings in the two principal directions of an in-plane specimen.

In order to carry out successfully an equibiaxial tensile test, several devices have been proposed so far. The most common experiment carried out in order to obtain an equibiaxial tension test was the stretching of a balloon, thereby swelling of a disk maintained on

its circumference and then further radial traction of this disk according to Nottin [16]. The main advantages and disadvantages of such devices are discussed as follows:

- Swelling of a balloon [2,3]: According to the authors such devices allow one to obtain an almost perfect equibiaxial state of deformation. However, instabilities occur at large deformation as per Alexander [3]. Moreover, this device allows equibiaxial tension only and the manufacturing cost of the specimen is very critical.
- Swelling of a disk maintained on the circumference of a cylinder [13–15]: This solution seems to be effective, although the state of biaxiality is valid only at the top of the inflated disk—this may induce the problem of strain measurement. However, on one hand, such a system does not make it possible to carry out a biaxial tension test with different intensities of stretching in the two directions of traction; on the other hand, maintaining the swelling of a disk on its circumference requires the use of a specific hydraulic system and thus the cost of testing is exorbitant.
- Swelling and traction of a cylinder [12]: This solution is also very effective. However, it also has the two main drawbacks of the previous mechanisms: manufacturing the specimen is difficult and the cost of the device and testing is expensive.
- Traction of a squared plate on its side [7–9]: This solution also provides good results and the specimens are simple to manufacture. The mechanism allows non-equibiaxial tension tests; however, in its present version the mechanism is a specific one and requires two different motors for both directions of tension, thereby creating a costly mechanism.

The New Biaxial Tension Mechanism

A new low cost biaxial test mechanism is hereby proposed which is capable of producing either equibiaxial or non-equibiaxial tension on any in-plane specimen. In order to take advantages of the solution proposed by Obata et al. [7] and Kawabata et al. [8,9], and to further reduce the cost of the mechanism and ultimately the specimen testing, the proposed mechanism was conceived. Moreover, this mechanism is adaptable to any uniaxial tension machine since such a machine exists in almost all of the mechanical engineering laboratories.

The mechanism is adapted on a uniaxial tension machine INSTRON 4302 as shown in Fig. 1.

The system was conceived in order to be able to carry out cyclic biaxial tension tests in large deformation with stretching in the two directions of tension with a possibility of different load ratios as shown in Fig. 2. The different features of the mechanism are described in Table 1.

The base of the mechanism (Part 1) as shown in Fig. 2 is fixed on the bottom of the tensile machine, while the upper half (Part 2) is fixed on the moving crosshead of the machine.

When the moving crosshead of the tensile machine is displaced, the higher vertical grip fixed on moves accordingly; whereas, the lower vertical grip fixed at the base plate of the tensile machine remains motionless which is identical to any uniaxial testing.

The horizontal grips are fixed to two horizontal draw bars (Part 5) which in turn are attached to the upper half and lower base through six links as shown in Fig. 3. Two of these bars are linked to the moving crosshead of the tensile machine through two plates (Part 9) which are hinged to the bottom and also linked to the moving crosshead of the tensile machine as shown in Fig. 3. Thus, the horizontal drawbars remain on the median of the segment formed by the vertical grips. On the other hand, the horizontal draw bars are connected to a sliding bush bearing as shown in Fig. 4, which glides on an oblique bar (Part 8) for providing a straight line adjustment of the horizontal displacement as shown in Fig. 4.

In this way, when the moving crosshead goes up, the vertical

FIG. 1—*Biaxial mechanism on uniaxial tension machine* (*INSTRON 4302*).

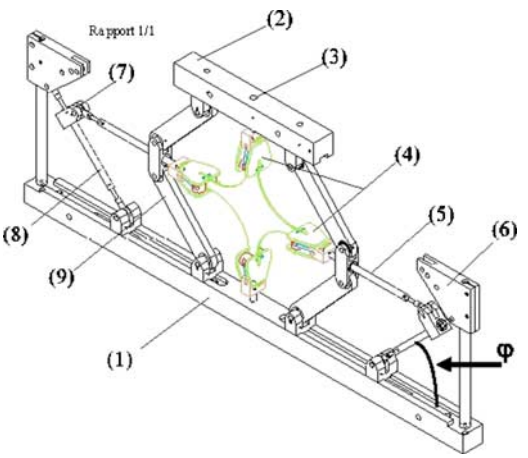

FIG. 2—*Schematic layout of the biaxial tensile test mechanism.*

TABLE 1—*Description of the main parts of the mechanism.*

Part No.	Description
(1)	Fixed crosshead
(2)	Moving crosshead
(3)	Vertical draw bar (2 bars)
(4)	Self-tightening grips (4 clamps)
(5)	Horizontal draw bar (2 bars)
(6)	Part of adjustment of the ratio of stretching between vertical and horizontal directions (2 parts)
(7)	Bush bearing (2)
(8)	Adjustment bars of the ratio of stretching between vertical and horizontal directions (2 bars)
(9)	Plate (2)

grip moves with a velocity "v," whereas, the vertical bottom grip is motionless. During this time, the horizontal grips move up with a velocity of "$v/2$" and simultaneously move in the horizontal plane with a velocity of "h" and go into opposite directions (reverse front walk).

The relation between v and h is given by the angle "φ", which is formed by the oblique bars with the horizontal. The part of adjustment (Part 6) as shown in Figs. 2 and 4 makes it possible to vary φ in order to get different stretch ratios.

$$\tan\varphi = 1,2,3 \text{ or } 4 \Leftrightarrow \begin{cases} \text{equibiaxial tension } (r=1)\text{: } h=v \\ \text{biaxial tension } (r=3)\text{: } h=3v \\ \text{biaxial tension } (r=2)\text{:} h=2v \\ \text{biaxial tension } (r=4)\ h=4v \end{cases} \tag{8}$$

where h and v are the horizontal and vertical displacements and r is the ratio between these displacements ($r=h/v$).

In this way, the stretch obtained by such a mechanism could be related to:

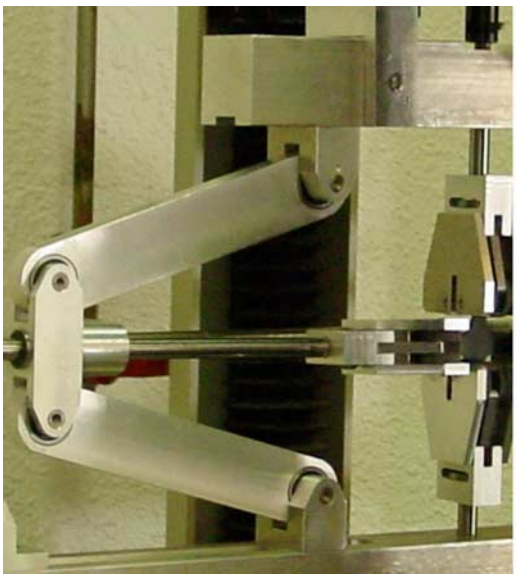

FIG. 3—*Adjustment of the vertical displacement of the horizontal grips.*

FIG. 4—*Adjustment of the horizontal displacement of the horizontal grips.*

$$\lambda \text{ and } \beta = 1 + \frac{\lambda - 1}{r} \tag{9}$$

where λ and β are the strains in the vertical and horizontal directions.

The stress measurement is carried out in the following way. As the vertical top grip is fixed to the load cell through the vertical draw bar (Part 3), the link between this grip and the load cell makes it possible to obtain a measurement of the stress in the vertical direction.

As the two horizontal grips are fixed on the horizontal draw bars (Part 5), the biaxial specimen arm is instrumented with rosette strain gages in order to measure the strain in the horizontal direction of tension as per Asch [32]. Thus the strains in both the vertical and horizontal directions are thereby evaluated. From these strains the stress is calculated indirectly.

A Biaxial Tension Test Specimen

As no standard is available concerning the biaxial tension experiment in large deformation, and more particularly on the specimen dimensions, it is advisable to carefully define dimensions of the sample used. In order to validate the specimen, numerical simulations of biaxial loading for large deformation have also been carried out. Because of the grips, the specimen thickness has to be less than 5 mm.

Due to the size and limits of the biaxial mechanism, the specimen mounted in the grips has to be uniformly gripped during the test and no slippage is allowed for which a tightening length on the grip is kept as 5 mm for a square specimen of 60 mm at the beginning of the load to 240 mm at the end. This indicates a total stretch of 180 mm in both directions. To reach the highest rate of deformation, specimen dimension contained in the minimum square region of interest is observed at the beginning of the test. The dimensions of a sample are defined in Fig. 5.

The dimension of the specimen is directly related to the blending radius R. R must be given in order to guarantee biaxial loading in the center of the specimen. Numerical simulations, illustrated in Fig. 6, have been carried out for various values of R. The simula-

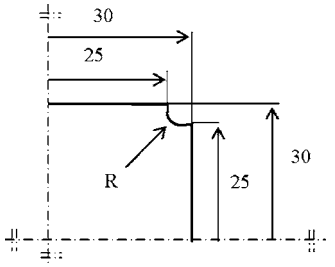

FIG. 5—*Dimensions of the specimen for biaxial tension* (*in mm*).

tions have been carried out using Finite Element Code Modulef. All the simulations have been performed for large strain, considering the behavior presented Eq. 5.

Such simulations have revealed that, even for large deformation, strains were still biaxial or equibiaxial on the center of the sample for any value of *R*, as shown in Figs. 7–10.

Figures 7–10 also show that displacements, and thus deformations are much more important near the grips than in the center of the specimen. The area close to the grips is submitted only to uniaxial tension and the strains are thus bigger, inducing smaller deformation in the center of the specimen. For this reason, in order to reach the higher level of strain in the center of the specimen, a radius *R* equal to 5 mm was finally chosen.

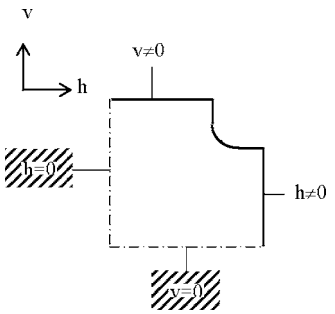

FIG. 6—*Boundary conditions for numerical simulations of the specimen for biaxial tension.*

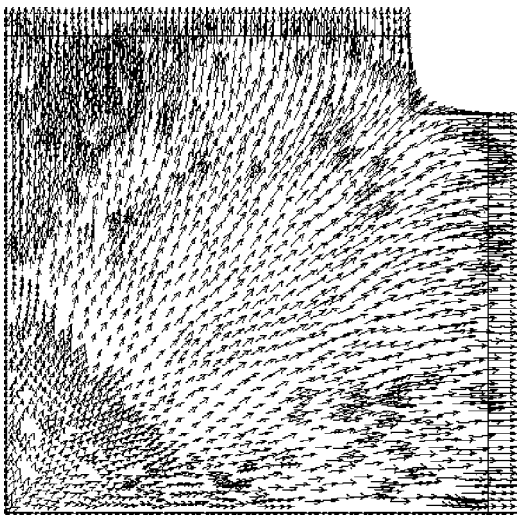

FIG. 7—*Displacement fields for* R = 1 *and* 90 mm *of displacement imposed on the grips of both directions.*

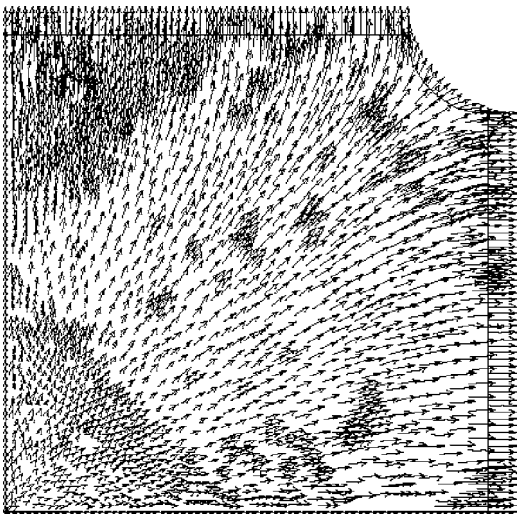

FIG. 8—*Displacement fields for* R = 5 *and* 90 mm *of displacement imposed on the grips of both directions.*

Video Extensometer

In order to perform the test and to obtain a relevant measurement of the strain in the center of the specimen a video extensometer was used.

The principle of this video extensometer is to focus a camera on the studied deformation zone at the center of the specimen where four points have been plotted. Software analyzes in real time the displacement of the four points in order to calculate the longitudinal and the transverse strains within the specimen. This information is then used in order to control the speed of the cross head of the tension machine to guarantee the vertical strain rate to be constant. The deformations are measured simultaneously in the vertical and horizontal directions. This video extensometer gives the two strains that are compared in Fig. 11 for different values of corner radius of the specimen which proved that the relations, Eqs. 8 and 9, imposed by the mechanism, are verified on the local vertical and horizontal strains. The result reveals that the expected ratio between the vertical and the horizontal deformations is satisfied with a good agreement.

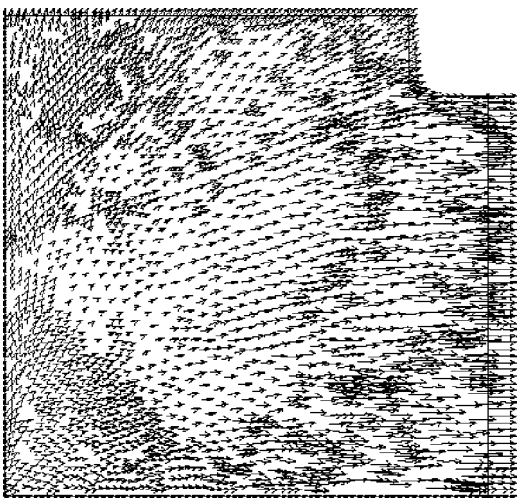

FIG. 9—*Displacement fields for* R = 1 *and* 90 mm *of displacement imposed on the horizontal grips and* 22.5 mm *on the vertical ones.*

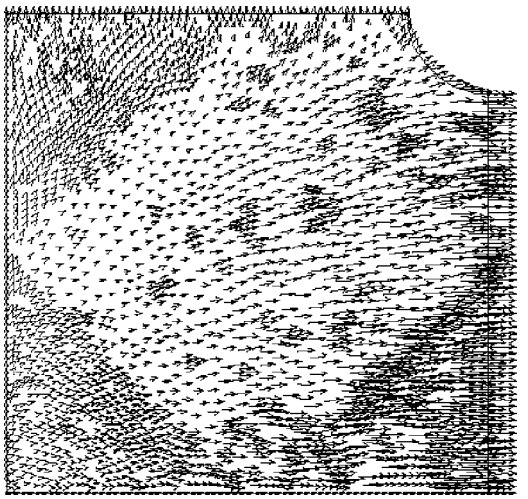

FIG. 10—*Displacement fields for* R=5 *and* 90 mm *of displacement imposed on the horizontal grips and 22.5 on the vertical ones.*

Experimental Results and Behavior Laws Comparison

All of the experimental tests have been conducted at a constant strain rate $\dot{\lambda}=10^{-3}$. The considered thickness of the specimen is 2 mm. Specimens have been punched out using a die from a calendered sheet of rubber.

Biaxial Tension Tests

As the proposed biaxial mechanism is constituted of rigid bars and not of belt, cyclic loadings are easy to carry out. Figure 12 presents a cyclic equibiaxial tension test. Figure 13 presents biaxial tension tests for all ratios *r*, defined by Eq. 8, available for the proposed mechanism and uniaxial tension test carried out on the tension machine. The presented results are the loading part of the second cycle.

Identification of the Behavior

In order to highlight the performances of the new biaxial mechanism, two different rubber-like materials were studied. A natural rubber (NR) and a polychloroprene rubber (CR) both were reinforced with particles of carbon black. In order to neglect the Mullins effect [33], the response of materials on the second loading only is presently considered. Parameters of the strain energy density functions introduced in Eqs. 5 and 6 are thereby calculated. A least square root method is used for both models directly on the two-tension test for the Harth-Smith model, Eq. 5, and using the method proposed by Lambert-Diani and Rey for their model, Eq. 6. The evaluated coefficients are given in Table 2.

Figures 14 and 15 show a comparison of the evaluated strain energy densities and the experiments in the case of a uniaxial tension test and an equibiaxial tension test. As Figs. 14 and 15 reveal that both the models give good results in agreement with the experimental data and also for both the considered materials (NR and CR). Such strain energy densities functions are known to be very good results and such a result is not a surprise.

However, the results are in good agreement also because both the uniaxial and equibiaxial tension tests were used for parameter identification. In such conditions, if the selected strain energy densities were able to fit well the uniaxial tension test and equibiaxial

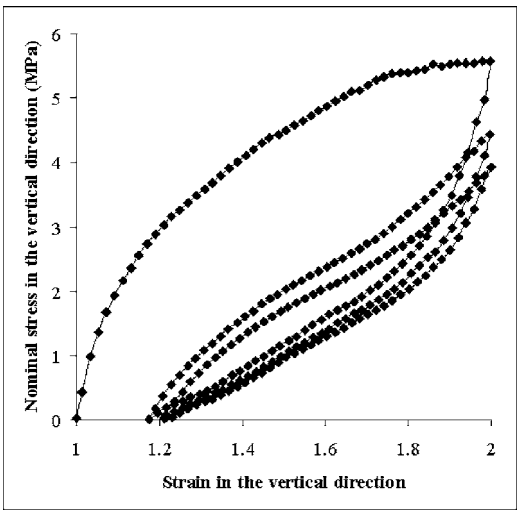

FIG. 12—*Cyclic equibiaxial tensile test for polychloroprene rubber.*

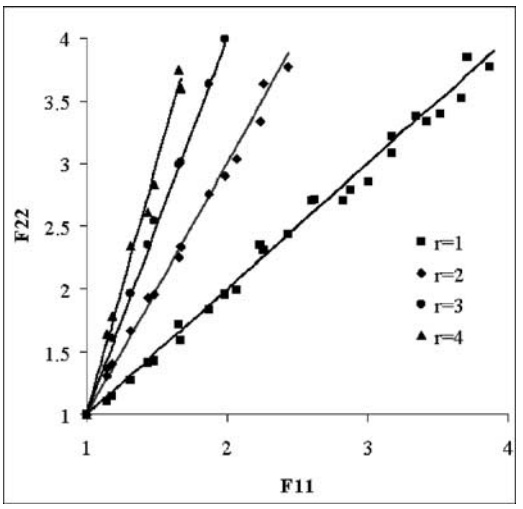

FIG. 11—*Comparison of the horizontal deformation* (*F22*) *versus the vertical deformation* (*F11*)—lines=theoretical *values;* dots=experimental *values.*

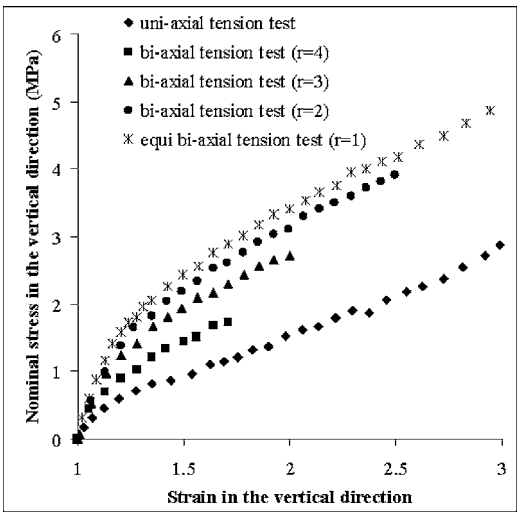

FIG. 13—*Biaxial tensile tests for natural rubber reinforced by particles of silica.*

TABLE 2—*Evaluated coefficients for strain energy density functions Eqs. 5 and 6 for NR and CR.*

	NR	CR
Harth-Smith density, Eq. 5	C_1=0.26482 MPa; C_2=0.31265 MPa; C_3=0.00232	C_1=1.04144 MPa; C_2=0.57721 MPa; C_3=0.00934
Lambert-Diani and Rey density, Eq. 6	$\exp(\alpha_0)$=0.2721 MPa; α_1=0.0123; α_2=0.0014; $\exp(\beta_0)$=1.4495 MPa β_1=−1.5159	$\exp(\alpha_0)$=0.8562 MPa; α_1=1.426; α_2=−0.0089; $\exp(\beta_0)$=6.5627 MPa; β_1=−1.8161

tension test, and if the identification method used is efficient, the comparison between experiment and models has to be good. Therefore, a third test, which has not been used to identify the parameters of each function, has to be used to validate, or not, the chosen strain energy densities functions.

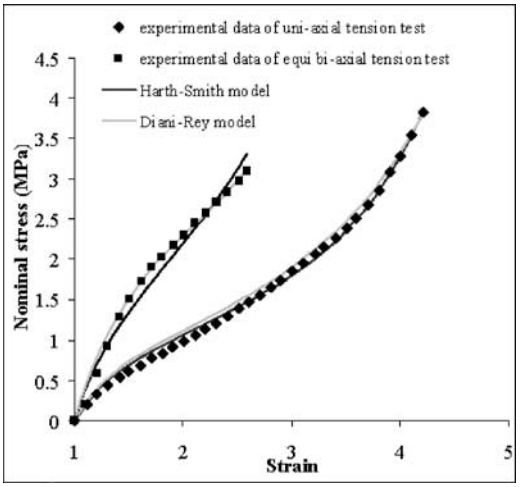

FIG. 14—*Comparison of Harth-Smith model, Eq. 5, and Lambert-Diani and Rey model, Eq. 6, with the experiment for NR.*

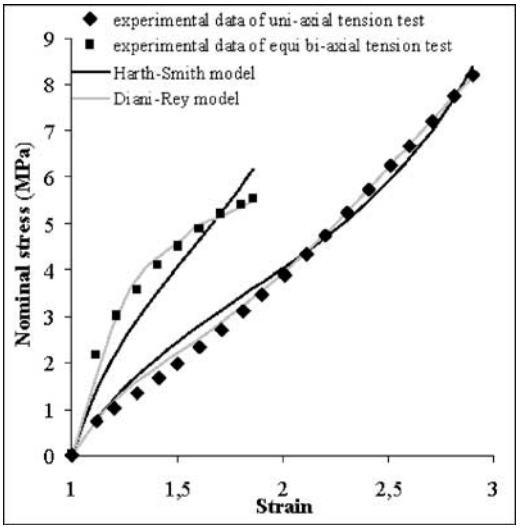

FIG. 15—*Comparison of Harth-Smith model, Eq. 5, and Lambert-Diani and Rey model, Eq. 6, with the experiment for CR.*

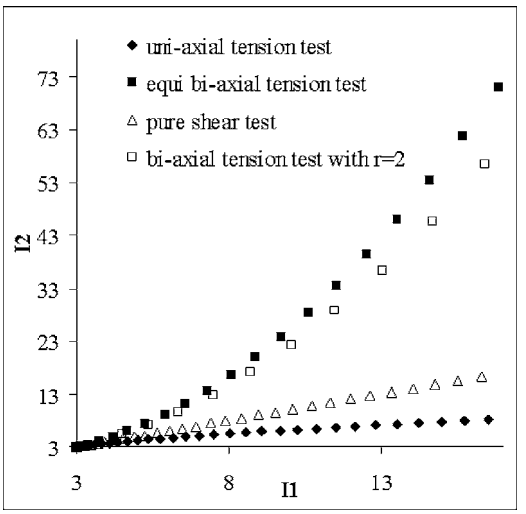

FIG. 16—*Variation of I_2 with respect to (w.r.t.) I_1 for uniaxial, equibiaxial, and biaxial (r=2) tensile tests and pure shear test.*

Validation of the Proposed Models

In order to validate the identification, and more specifically, the proposed models, Eqs. 5 and 6, identified on two different loading cases, it is classical to use the identified strain energy density to predict the response of the materials on a third loading case.

The most common third loading case used to validate the strain energy is a pure shear test (PS). However, the PS induces very few variations of the second invariant I_2 in regard to the first one I_1 and the response is very close to the unixial tension test, as shown in Fig. 16. As such, this test might not be very efficient to validate the identified strain energy density.

One of the advantages of the proposed mechanism is to allow biaxial tension tests, which are not equibiaxial ones. In such a case, the variations of I_2 with respect to I_1 is important as the difference between equibiaxial tension or uniaxial tension and nonequibiaxial tension will be enough to validate, or not, the governing model.

In the case of biaxial tension:

$$T_{11}^{BT} = 2\left(\frac{\partial W}{\partial I_1}\left(\lambda - \frac{1}{\lambda^3\beta^2}\right) + \frac{\partial W}{\partial I_2}\left(\lambda\beta^2 - \frac{1}{\lambda^3}\right)\right) \qquad (10)$$

where λ and β are, respectively, the deformation in the vertical and horizontal directions, as defined in Eq. 9.

Figures 17 and 18 give a comparison of the identified proposed models with the experiment data in the case of a biaxial tension test with r=2.

As seen in Figs. 14 and 15, both the proposed models gave a very satisfactory result for the uniaxial and equibiaxial tension test for the identification of governing models. However, when the third loading case was applied, which induces a large variation on both invariants in order to see the influence of each derived part of the strain energy density function, as shown in Figs. 17 and 18, the results are no longer the same.

These types of results allow one to improve the different strain energy density function and it is noticed that the model proposed by Diani and Rey [12] is closer to the experimental data as compared to the Hart-Smith model.

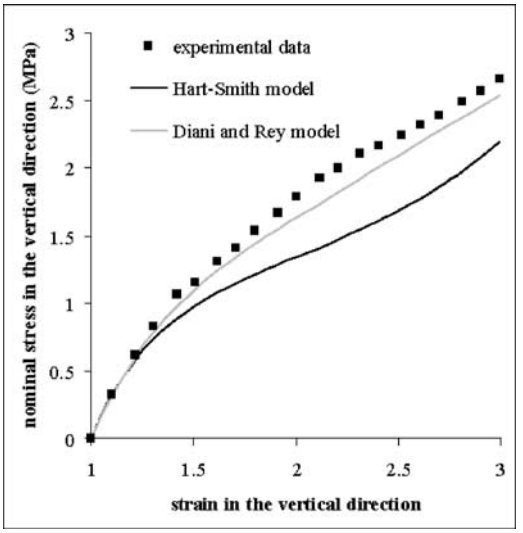

FIG. 17—*Comparison of the proposed models with experiment on a biaxial tension test* (r=2) *for NR.*

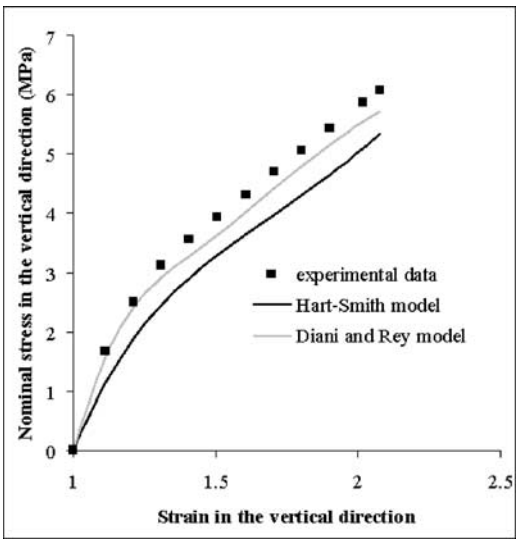

FIG. 18—*Comparison of the proposed models with experiment on a biaxial tension test* (r=2) *for CR.*

Conclusion

This paper deals with the development of a new mechanism of biaxial tension. This mechanism appears to be very useful according to the results it provides for the validation of theoretical models. With such a mechanism one can carry out an equibiaxial tension test and also a biaxial tension with different deformation in both directions. The experimental results reveal the utility and the accuracy of a chosen strain energy density and its identification to model the behavior of a rubber-like material as a sample case. The same may be true to model the behavior of fiber-reinforced composites that may be either orthotropic or anisotropic in nature. Furthermore, this mechanism also allows cyclic biaxial loadings at a very low cost which can be adapted to any existing uniaxial tensile testing machine.

References

[1] Rivlin, R. S., "Large Elastic Deformations of Isotropic Materials: I. Fundamental Concepts, II. Some Uniqueness Theorems for Pure Homogeneous Deformations," *Philos. Trans. R. Soc. London, Ser. A*, Vol. 240, 1948, pp. 459–490.

[2] Harth-Smith, L. J., "Elasticity Parameters for Finite Deformations of Rubber-like Materials," *Z. Angew. Math. Phys.*, Vol. 17, 1966, pp. 608–625.

[3] Alexander, H., "Tensile Instability of Initially Spherical Balloons," *Int. J. Eng. Sci.*, Vol. 9, 1971, pp. 549–563.

[4] Ogden, R. W., "Large Deformation Isotropic Elasticity on the Correlation of Theory and Experiment for Incompressible Rubber-like Solids," *Proc. R. Soc. London*, Vol. A326, 1972, pp. 565–579.

[5] Treoloar, L. R. G., "Stress-strain Data for Vulcanized Rubber Under Various Types of Deformation," *Trans. Faraday Soc.*, Vol. 40, 1944, pp. 59–70.

[6] Rivlin, R. S. and Saunders, D. W., "Large Elastic Deformations of Isotropic Materials. Experiments on the Deformation of Rubber," *Philos. Trans. R. Soc. London, Ser. A*, Vol. 243, 1951, pp. 251–288.

[7] Obata, Y., Kawabata, S., and Kawai, H., "Mechanical Properties of Natural Rubber Vulcanizates in Finite Deformation," *J. Polym. Sci. A*, Vol. A28, 1970, pp. 903–919.

[8] Kawabata, S. and Kawai, H., "Strain Energy Density Functions of Rubber Vulcanizates from Biaxial Tension," *Adv. Polym. Sci.*, Vol. 24, 1977, pp. 90–124.

[9] Kawabata, S., Matsuda, M., Tei, K., and Kawai, H., "Experimental Survey of the Strain Energy Density Function of Isoprene Rubber Vucanizate," *Macromolecules*, Vol. 14, 1981, pp. 154–162.

[10] Fukahori, Y. and Seki, W., "Molecular Behaviur of Elastomeric Materials Under Large Deformations: I. Re-evaluation of the Mooney-Rivlin Plot," *Polymer*, Vol. 33, 1991, pp. 502–508.

[11] Lambert-Diani, J. and Rey, C., "New Phenomenological Behavior Laws for Rubbers and Thermoplastic Elastomers," *Eur. J. Mech. A/Solids*, Vol. 18, No. 6, 1998, pp. 1027–1043.

[12] James, H. M. and Guth, E., "Theory of the Elastic Properties of Rubber," *J. Chem. Phys.*, Vol. 11, 1966, pp. 455–481.

[13] De Vries, A. J., and Bonnebat, C. "Uni and Biaxial Stretching of Chlorinated PVC Sheets. A Fundamental Study of Thermo Deformability," *Polym. Eng. Sci.*, Vol. 16, No. 2, 1976.

[14] Roberts, B. J. and Benzies, J. B., "Relationship Between Uniaxial and Equibiaxial Fatigue in Gum and Carbon-black Filled Vulcanizates," *Plastics and Rubber: Materials and Applications*, Vol. 3, No. 2, 1978, pp. 49–54.

[15] Bhate, A. P. and Kardos, J. L., "A Novel Technique for the Determination of High Frequency Equibiaxial Stress-deformation Behavior of Viscoelastic Elastomers," *Polym. Eng. Sci.*, Vol. 24, No. 11, 1984.

[16] Nottin, J. P. and Racimor, P., "Mechanical Behavior of Solid Propellants During Tensile Tests with Variable Temperature," *AIAA J.*, 1989.

[17] Mullins, L. and Tobin, N. R., "Theorical Model For Elastic Behavior of Reinforced Vulcanized Rubbers," *Rubber Chem. Technol.*, Vol. 30, 1947, pp. 551–571.

[18] Mullins, L., "Softening of Rubber by Deformation," *Rubber Chem. Technol.*, Vol. 42, 1969, pp. 339–362.

[19] Larraba, A., "Etude des comportements hyperélastiques de

deux élastomères de type NR et PDMS," Ph.D. Ecole Nationale Supérieure des Mines de Paris, 2000.
[20] Anand, L. A., "A Constitutive Model for Compressible Elastomeric Solids," *Comp. Assist. Mech. Eng. Sc.*, Vol. 18, 1996, pp. 335–339.
[21] Treoloar, L. R. G., *The Physics of Rubber Elasticity*, 3rd ed., Oxford University Press, Oxford, 1975.
[22] Mark, J. E. and Erman, B., *A Rubber-like Elasticity, A Molecular Primer*, Wiley, London, 1987.
[23] Wang, M. C. and Guth, E., "Statistical Theory of Networks of Non-Gaussian Flexible Chains," *J. Chem. Phys.*, Vol. 20, 1952, pp. 1144–1157.
[24] Treoloar, L. R. G., and Riding, G., "A Non-Gaussian Theory for Rubber in Biaxial Strain. I. Mechanical Properties," *Proc. R. Soc. London*, Vol. A369, 1979, pp. 261–280.
[25] Arruda, E. M. and Boyce, M. C., "A Three-dimensional Constitutive Model for the Large Stretch Behavior of Rubber Elastic Materials," *J. Mech. Phys. Solids*, Vol. 41, 1993, pp. 389–412.
[26] Wu, P. and Van Der Giessen, E., "On Improved 3-D Non-Gaussian Network Models for Rubber Elasticity," *Mech. Res. Commun.*, Vol. 19, 1992, pp. 427–433.
[27] Diani, J., Brieu, M., and Vacherand, J. M., "A Damage Directional Constitutive Model for Mullins Effect with Permanent Set and Induced Anisotropy," *Eur. J. Mech. A/Solids*, Vol. 25, No. 3, 2006, pp. 483–496.
[28] Diani, J., Brieu, M., and Gilormini, P., "Observation and Modeling of the Anisotropic Visco-hyperelastic Behavior of a Rubber-like Material," *Int. J. Solids Struct.*, Vol. 43, No. 10, 2006, pp. 3044–3056.
[29] Diani, J., Brieu, M., Vacherand, J. M., and Rezgui, A., "Directional Model for Isotropic and Anisotropic Hyperelastic Rubber-like Materials," *Mech. Mater.*, Vol. 36, 2004, pp. 313–321.
[30] Mooney, M., "A Theory of Large Elastic Deformation," *J. Appl. Phys.*, Vol. 11, 1940, pp. 582–592.
[31] Ogden, R. W., *Nonlinear Elastic Deformations*, Ellis Hardwood, Chichester, 1984.
[32] Ash, G., *Les capteurs en instrumentation industrielle*, 5th Ed., Dunod, Paris, 1999.
[33] Mullins, L., "Softening of Rubber by Deformation," *Rubber Chem. Technol.*, Vol. 42, 1969, pp. 339–362.